ISSN: 3067-2317
Research Article

World Journal of Artificial Intelligence and Robotics Research

Applying Artificial Intelligence to Distributed Generation in Local Networks

Carlos Armenta-Déu[1*]

DPT. Matter Structure, Thermal Physics and Electronics and Faculty of Physics, Complutense University of Madrid, 28040 Madrid (Spain)

***Corresponding author:** Carlos Armenta-Déu, DPT. Matter Structure, Thermal Physics and Electronics, Faculty of Physics, Complutense University of Madrid, 28040 Madrid (Spain).

Submitted: 13 February 2025 **Accepted:** 19 February 2025 **Published:** 27 February 2025

https://doi.org/10.63620/MK.WJAIRR.2025.1011

Citation: *Armenta, Déu., C. (2025). Applying Artificial Intelligence to Distributed Generation in Local Networks. Wor Jour of Arti inte and Rob Res, 2(1), 01-20.*

Abstract

The paper describes the application of artificial intelligence to the operation and energy management of a local network consisting of a group of interconnected households operating as a distributed generation system for electric power and a district heating system for thermal energy.

The proposed Artificial Intelligence Protocol (AIP) helps a control unit to manage power supply from renewable sources with the aim of a null energy balance for the local network, avoiding grid dependence and optimizing the system energy performance. The AIP selects the most efficient power source for power supply and energy exchange throughout the local network.

The AIP achieves the null energy balance by adjusting operational parameters to regulate the output power for the individual household installation and the energy distribution network. The AIP is applied to a group of unbalanced electric and thermal energy households, configuring a local network with an electric distributor and a heating ring to exchange electric and thermal energy between houses.

The AIP application to this local network results in an accurate prediction of electric power generation, higher than 99.7%, showing a global deviation of 0.1 kWh/day. Null energy balance prediction is highly accurate, 97.1%, with a maximum daily deviation of 9.61 kWh/day out of 209 kWh/day energy exchanged corresponding to thermal losses.

Introduction

Implementing renewable energy installations in the residential sector to reduce energy dependence on electricity generated by fossil fuel power plants and gas supply has led to a new scenario in the energy distribution frame [1-3]. The classical electric household layout is a private installation with the power supply to the own house, releasing the excess of generated electricity, if any, to the grid [4-6]. Thermal energy generated in private renewable energy installations like solar thermal collectors, low enthalpy systems, or biomass micro-plants operate in a single direction with no exchange to the community distribution network [7-16].

Residential thermal and electric power generation from renewable energy installations are not balanced throughout the day because of the variability in renewable resources and energy consumption [17-19]. The unbalanced consequence is exchanging the excess of generated energy, thermal or electric, to a storage system or an external network [20-22]. In the case of electricity, the solution is less complex since we can exchange electric energy excess with the grid or store it in batteries [23-25]. Nevertheless, thermal energy excess suffers from the lack of exchanging methods to a global distribution system or the storage system's low duration.

Electric energy storage requires an additional investment since batteries are expensive, especially lithium type, and periodical replacement due to the continuous battery degradation with use. On the other hand, batteries require maintenance and additional space, which is not always available in households. The need for a special inverter/charger unit adds extra cost to the installation, generating the rejection of many users regarding using a storage system. Furthermore, the payback period for batteries can be too long, discouraging their implementation by installers and users [26-28].

Grid connection has become a current alternative for the energy excess in electric household generation; nevertheless, the low fare the electric companies pay for the electricity grid injection reduces the householders' interest in selling energy to the grid, especially if we consider the extra cost for the specific equipment to warranty the quality of the injected electric signal. In this scenario, the renewable energy system lowers its power generation capacity, reducing the energy efficiency and the payback time [29-30].

Thermal energy shows a similar state of the art with the noticeable difference that energy storage lasts for a short time, currently no longer than 24 hours; therefore, we should consume the household thermal generation from renewable energies within a day; otherwise, it is useless. Another significant difference with electric energy is the impossibility of exporting energy to a global network since this option is not feasible today.

Household renewable energy generation can be considered a distributed power plant of small size; therefore, we can design a local network connecting every installation with every single installation acting as an individual power source. This configuration allows the power excess distribution, thermal and electric, depending on the household energy balance. The electric link is a local grid with individual two-way connections to a central distributor, and the thermal network acts as a low-size district heating [31-37].

Thermal and electric energy distribution in a local network cannot depend on human beings for multiple reasons: errors in managing the energy distribution, inappropriate training, lack of attention, and continuous operation with no breaking time, etc.; therefore, the system requires automation and programming to operate at optimum conditions with the highest efficiency possible. Automation avoids human dependence and guarantees good servicing at all times, while programming assures the energy supply at specific time intervals during the day [38-41].

This configuration, however, does not properly operate if human habits change, altering the household energy balance and the programmed sequence of thermal and energy exchange with local electric networks and district heating. We can solve this problem by applying artificial intelligence (AI) to the system operation since the AI adopts a variable working protocol that accommodates every single household energy balance.

Artificial Intelligence Application

Artificial Intelligence is practical in configurations like the one described above since it follows an adaptive protocol that learns from human habit variation by adjusting the operational conditions to the current status of the energy balance [42-44]. We could avoid the use of AI if we translate any change in daily habits regarding energy consumption to the programmed protocol for electric or thermal energy exchange; however, people are very busy with daily tasks and forget to make necessary changes in the protocol, or they don't know how to manage the situation. The principal consequence of mismatching the current energy balance by the setup protocol is the need to consume energy from the grid or gas distribution network and the energy efficiency reduction.

Artificial Intelligence supports the control system that operates the local electric network and the district heating; the control unit evaluates the energy balance for every household and determines the energy exchange between houses based on energy efficiency and maximum power availability. Figure 1 shows a graphic representation of the local electric network and district heating used as a model for the AI application.

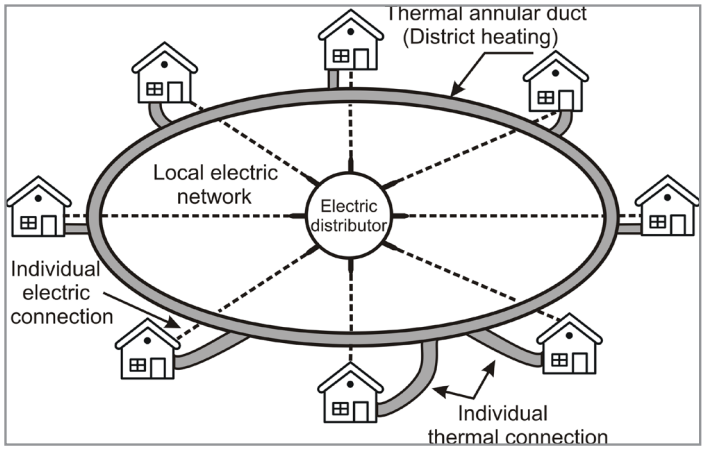

Figure 1: Layout of local network

Control Unit and Artificial Intelligence

Control unit (CU) based on artificial intelligence operates as follows:

- CU collects power generation and energy consumption data from renewable sources and household energy meter. This operation is made for every single house.
- CU determines the instantaneous energy balance of each home and classifies them into deficit and surplus types.
- CU evaluates the power transfer from surplus to deficit installation type and proceeds with the energy exchange based on null energy balance at the end of the process, if possible, or minimum deficit for the deficit installation type. The en-

ergy exchange considers minimizing power losses during the process.

- CU records instantaneous power transfer amount and origin and destination, creating a database for future applications.
- CU develops the power transfer and energy exchange every day according to the database records.
- If energy balance changes due to random variations in power generation, the control unit reevaluates the energy balance for every household installation, prioritizing to achieve a null energy balance, if possible, by reducing non-essential energy consumption according to AI principles.
- In this former situation, the AI evaluates the critical energy consumptions based on previously recorded data from individual appliances.
- The AI protocol compares the recorded data with setup prioritize list and decides which energy consumptions are critical to maintain for a null energy balance in case the initial value is below zero. The prioritize list fulfils standard human habits.
- If the energy balance remains above zero after considering only critical loads, the AI protocol includes fundamental loads for energy balance calculation; if the energy balance continues above zero, the AI protocol moves to consider the ancillary loads.
- CU accommodates the power transfer and energy exchange according to the setup premise of null energy balance, if possible, or minimum deficit for the installation type.
- If energy consumption changes because of human habits variation, the AI protocol redefines the prioritize list according to the detected changes.
- The automatic application of AI protocol to control unit energy management can be commuted to manual operation by the user under specific circumstances like new appliances implementation, changes in setup comfort conditions, increasing household living people number, etc.
- This situation lasts for a short time until AI notices that it remains unchanged for a while; at this moment, the AI redefines its protocol and prioritize list to accommodate it to the new situation.

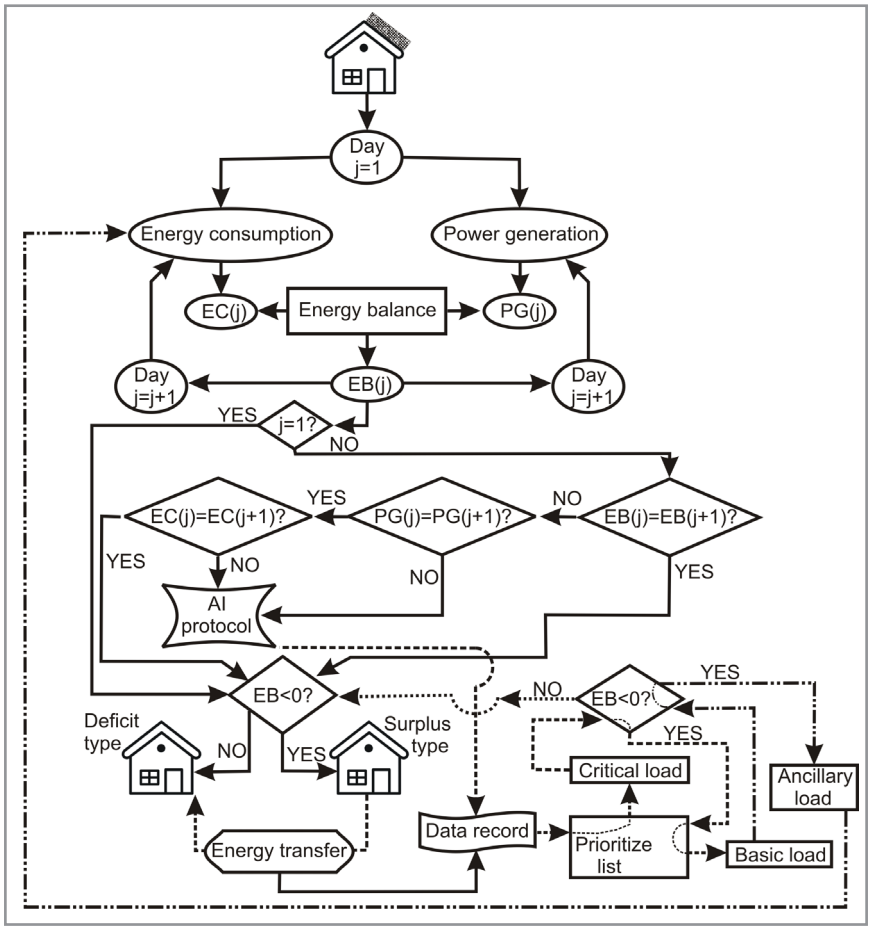

Figure 2: Flowchart of the System Operation Protocol

Local Network Configuration

The local network under study uses renewable energy sources to power households. Among the many current sources, the most currently used for heating and electricity in modern houses are solar thermal and photovoltaic, wind energy, biomass, and geothermal. Other sources like micro-hydro, wave, and tidal energy are scarce and difficult to implement in our homes.

Depending on the location, the above-mentioned renewable sources are available or not. For a more extended analysis, we

consider a local network configuration with all these sources implemented but not all installed in every house. Table 1 shows the renewable energy source distribution for a set of 8 houses according to the layout in Figure 1. Table 2 shows the peak power generation for every individual installation. We obtained data from a residential conglomerate, which was specially developed for the use of renewable energy resources to operate completely autonomously.

Table 1: B Peak Power Generation (Kw)

House	1	2	3	4	5	6	7	8
PV	---	---	4.0	4.0	2.0	9.0	---	---
W	3.6	1.22	---	1.5	6.0	---	---	---
ST	2.8	---	---	---	---	4.0	---	8.0
B	---	6.0	---	---	6.5	---	7.2	---
G	---	---	5.5	7.6	---	---	---	6.8
Thermal	2.8	6.0	5.5	7.6	6.5	4.0	7.2	14.8
Electric	3.0	1.5	2.4	4.2	6.0	8.0	0	0

Table 1: A Renewable Energy Source Distribution for the Local Network

House	1	2	3	4	5	6	7	8
PV	NO	NO	YES	YES	YES	YES	NO	NO
W	YES	YES	NO	YES	YES	NO	NO	NO
ST	YES	NO	NO	NO	NO	YES	NO	YES
B	NO	YES	NO	NO	YES	NO	YES	NO
G	NO	NO	YES	YES	NO	NO	NO	YES

Legend: St (Solar Thermal); PV (Photovoltaic); W (Wind); B (Biomass); G (Geothermal)

We notice that some houses only install thermal energy, houses 7 and 8, while all others install thermal and electric. The electric power generation distribution is variable, with some houses prioritizing photovoltaic, houses 3, 4, and 6, while others prioritize wind energy, houses 1, 2, and 5. Regarding thermal power generation, the distribution is also variable: houses 1 and 6 only have solar thermal, houses 2, 5, and 7 are only equipped with biomass installation, houses 3 and 4 only have geothermal, and house 8 has a balance thermal power generation between solar thermal and geothermal units.

Power Generation and Energy Consumption

The Artificial Intelligence application to the local network energy management requires the hourly daily distribution of thermal and electric energy for every house. Figure 3 shows the hourly electric energy consumption evolution for every residence. On the other hand, the accurate energy balance used by the AI protocol requires knowing the power generation distribution; therefore, we collect information on solar and wind power hourly distribution to evaluate the electric generation. Figure 4 shows the evolution of solar and wind power during the day.

Electric Energy

Solar power profile corresponds to a clear sky day on an average sunny location; the wind power profile is taken as a standard although the high variability in wind resource may cause considerable variation regarding the one shown in Figure 4.

The defined procedure calculates the hourly energy balance for every house to apply the AI protocol to the local network. The protocol decides whether or not a household installation is suitable for energy exchange depending on the calculated energy balance. Figure 5 shows the electric energy balance for individual household in the local network. Table 2 shows the energy daily balance distribution by individual house.

We notice that the daily electric energy balance for the local network is null, proving that the system can operate with no grid dependence provided the accurate energy exchange between household installations occurs.

Table 2: Electric Energy Daily Balance Distribution by Individual House

House					1	2	3	4	5	6	7	8
Day					48.8	-31.6	-22.8	-13.4	85.9	-17.9	-25.0	-23.8
	Hour											
	1	2	3	4	5	6	7	8	9	10	11	12
Network	18	27	13	27	-26	-32	14	-32	12	-46	45	39

	13	14	15	16	17	18	19	20	21	22	23	24
Network	7	27	27	26	20	17	-45	-13	14	38	-42	27

Values for the upper section of table 2 are expressed in kwh, while for the lower section are in wh.

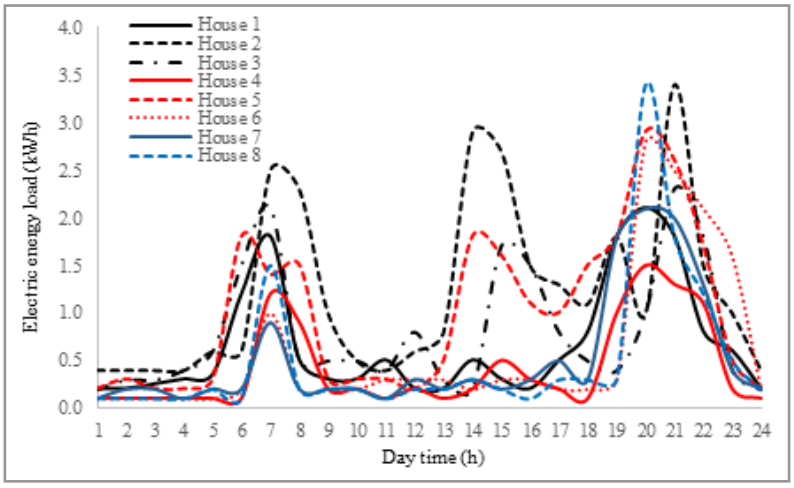

Figure 3: Individual Household Hourly Distribution of Electric Energy Consumption

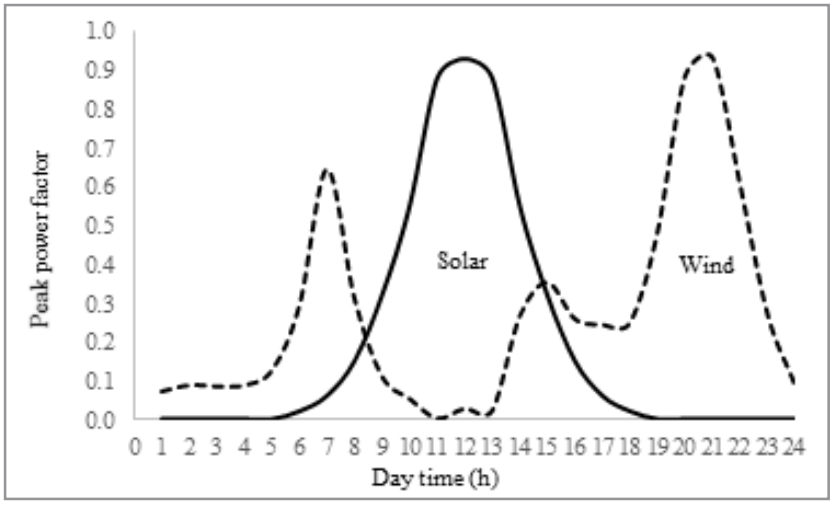

Figure 4: Solar and Wind Power Hourly Distribution

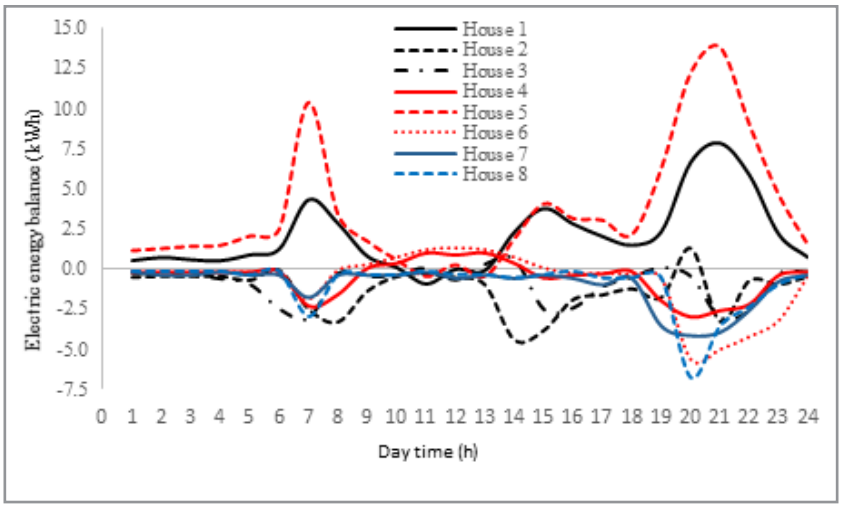

Figure 5: Individual Household Hourly Distribution of Electric Energy Balance

Analyzing data from Table 2, we notice that houses 1 and 5 are "energy producers" while the others are "energy consumers"; this particular configuration, derived from inefficient use of electric power generation, makes the local network especially useful for our purposes, such as the electric energy exchange between houses to avoid grid dependence, making energy consumption more efficient, and optimizing power resource use.

Analyzing data from Figure 5, we obtain that the daily hourly energy balance for the local network is negligible compared with the energy consumption, with a maximum ratio of 1.6%, meaning that the network operates based on a null energy balance. The residential conglomerate, regarding the type and peak power of renewable energy installations, responds to the private wishes of the householders, their purchasing power, and the available space in the household for renewable energy installation.

Thermal Energy

The required thermal energy for a household comprises sanitary hot water and building heating. The type and power of the thermal supply source are shown in Table 1. Figure 6 shows the daily distribution of solar thermal, biomass, and geothermal power supply.

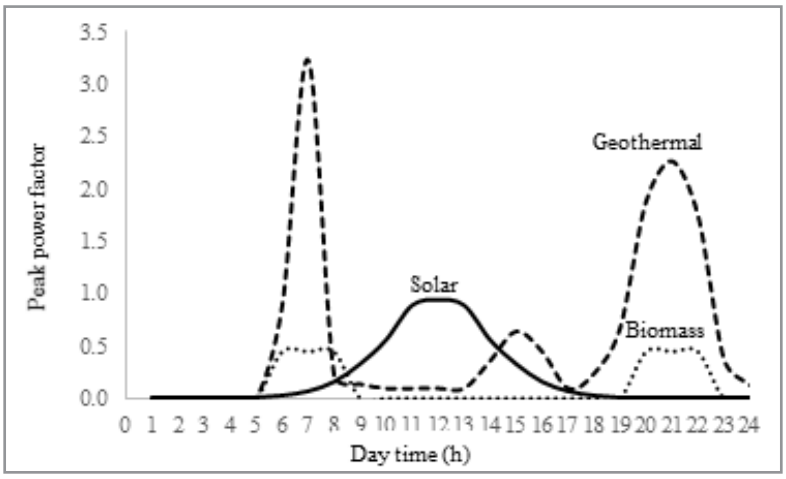

Figure 6: Solar, Biomass and Geothermal Power Hourly Distribution

Peak power factor for geothermal unit exceeds the 1.0 factor because it relates to the COP (Coefficient of Performance) value and not to the thermodynamic efficiency. As in the case of electric energy analysis, the defined procedure calculates the hourly energy balance for every house to apply the AI protocol to the local network. The protocol decides if a household installation requires energy exchange depending on the calculated energy balance. Figures 7 and 8 show the thermal energy consumption and balance for individual households in the local network. Table 3 shows the energy daily balance distribution by the single house.

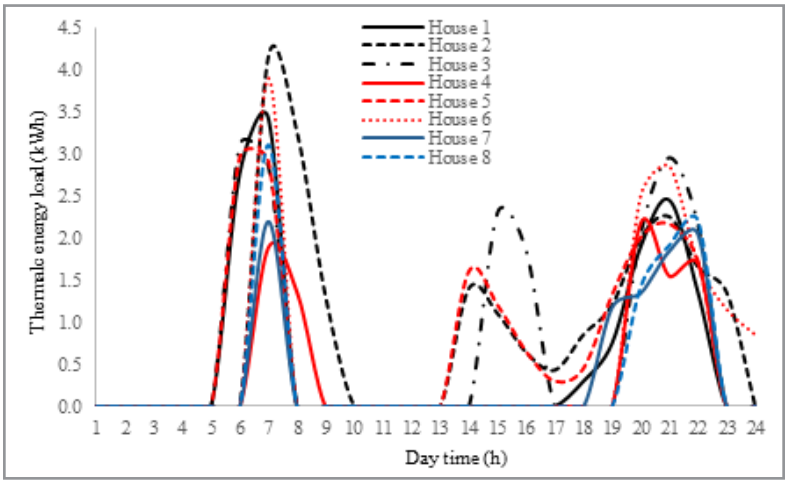

Figure 7: Individual Household Hourly Distribution of Thermal Energy Consumption

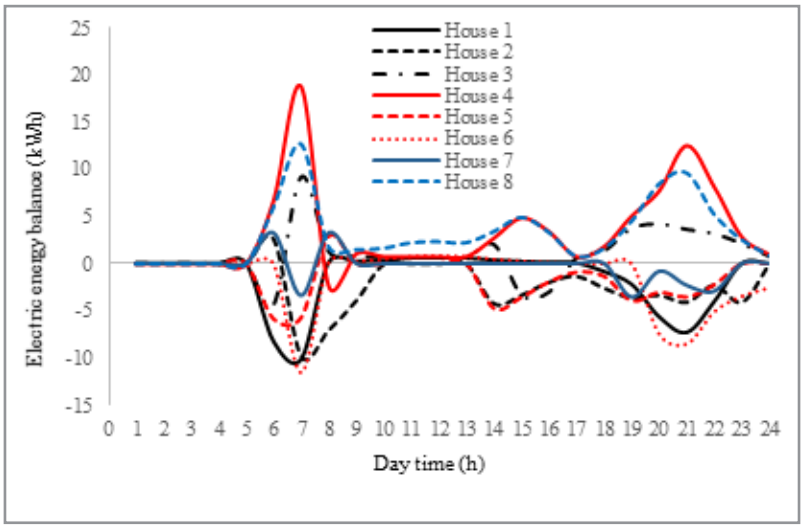

Figure 8: Individual Household Hourly Distribution of Thermal Energy Balance

Table 3: Daily Energy Balance Distribution by Individual House (Thermal) (kWh)

House					1	2	3	4	5	6	7	8
Day					-35.7	-48.5	23.6	78.3	-34.2	-34.4	-6.5	76.1
	Hour											
	1	2	3	4	5	6	7	8	9	10	11	12
Network	0	0	0	0	0	0	0	0	0	3.82	4.92	5.09
	13	14	15	16	17	18	19	20	21	22	23	24
Network	4.92	0	0	0	0	0	0	0	0	0	0	0

Analyzing data from Table 3, we realize that all thermal energy balances are null except for the hour interval between 10 a.m. and 1 p.m., where the balance is above zero, meaning the household group produces more thermal energy than needed. Disaggregating households with hourly energy balances above and below zero and grouping in positive and negative thermal energy balances, we have the next hourly distribution (Table 4).

Table 4: Disaggregated Thermal Daily Balance Distribution for Energy Deficit Cases (kWh)

	Hour											
	1	2	3	4	5	6	7	8	9	10	11	12
Network	0	0	0	0	0	-18.7	-40.7	-9.4	-3.9	0	0	0
	13	14	15	16	17	18	19	20	21	22	23	24
Network	0	-9.0	-10.3	-6.9	-2.2	-4.8	-13.4	-20.4	-25.8	-13.6	-7.5	0

Table 4 data show the thermal energy requirements by time interval due to households where energy demand exceeds thermal power generation; the deficit, according to data in Table 3 is compensated by the thermal energy surplus in the other households achieving a null energy balance for every hour except for the 10 a.m. to 1 p.m. period as mentioned before. Since thermal transfer causes higher energy losses than electric, we should consider to compensate for these losses by producing extra energy; this is the reason why the global daily thermal energy balance is above zero.

We estimate the thermal losses during heat transportation by applying the following equation:

$$\dot{Q}_L = U_L\left(\frac{\dot{Q}_t}{2} + T_d - T_{amb}\right) \quad (1)$$

Q_L are the thermal losses, Q_t is the heat flow transferred, U_L is the thermal losses coefficient, and T_{amb} and T_d are the ambient and household destination installation temperature?

Applying the current values for the selected local network results in an average value of 18.10 kWh. Comparing this value with the global thermal energy excess, 18.74 kWh, shown in the lower section of Table 3, we notice the AI protocol adjusts the heat flow thermal power generation to compensate for thermal losses with 96.6% accuracy. The slight difference between

global excess and thermal losses, 0.64 kWh/day, is negligible compared to the heat transferred throughout the local network, 0.34%.

Fundamentals

Household energy consumption depends on appliances' power and use time. Although it is hard to compute daily energy consumption because it requires an accurate record of element type power and time of use, the calculation simplifies due to the regular pattern humans follow in their daily activities. Indeed, with slight variations, people tend to develop daily tasks regularly at the same time during the same interval; therefore, the daily energy consumption corresponds to a standard value defined by the following expression:

$$\xi_d = \sum_{j=1}^{n} P_j t_j \tag{2}$$

P is the power, and t is the operating time of the appliance j.

The power generation derives from one or more renewable energy sources, according to the lower section of Table 1. Considering a general configuration with all the renewable power systems in the local network, we have:

$$\begin{aligned} \xi_{el} &= P_{PV}\, psh + P_w t_w^{ef} \\ \xi_{th} &= \eta_{th} GS + \dot{m}_b\, LHV + P_g^{el} COP \end{aligned} \tag{3}$$

ξ_{el} and ξth are the global electric and thermal energy generation, PPV is the photovoltaic array peak power, psh is the peak sun hours value, Pw is the wind turbine maximum power, t_w^{ef} is the time at which the wind turbine operates at maximum power, ηth is the solar thermal system efficiency, G is the solar radiation, S is the front surface of the solar collector, m_b is the biomass flow, LHV is the biomass low heating value, P_{gel} is the geothermal system electric power consumption, and COP is the coefficient of performance.

Since solar radiation evolves with day hour (Figure 4), the available hourly electric and thermal energy generation from solar radiation changes continuously according to Equation 3. On the other hand, the hourly solar radiation variation is influenced by the cloudiness index, reducing the solar radiation level and the power generation. In such conditions, the AI protocol should consider the predictable evolution of solar radiation according to a database for at least three consecutive years, the minimum period for accurate predictions; based on these data, the AI predicts electric and thermal power generation from solar radiation, and adjusts the operational mode to make the control unit setup the working parameters for a null energy balance and accurate electric and heat transfer. This operation is based on an AI protocol subroutine devoted to power source management.

A similar procedure applies to wind energy, based on collected data for at least one year. Regarding biomass, since no meteorological parameters influence the system performance, the regulation consists of adjusting the mass flow supply to control power generation. The AI protocol subroutine retrieves recorded data from past experiences for every household where biomass installation is available to achieve the null energy balance condition.

The artificial intelligence control on the geothermal system operation uses the PID curves for building heating, regulating the power generation by modifying the PID heating curve. Previous studies show that by regulating the PID curves, the power generation changes without affectation to critical parameters like the comfort temperature.

Combining equations 2 and 3, we have:

$$\begin{aligned} \xi_{el} &= \left(P_{PV}\, psh + P_w t_w^{ef}\right) t_{op} \\ \xi_{th} &= \left(\eta_{th} GS + \dot{m}_b\, LHV + P_g^{el} COP\right) t_{op} \end{aligned} \tag{4}$$

If energy demand remains constant but power generation changes because of solar radiation or wind speed variation, the artificial intelligence protocol adjusts parameters in Equation 4 to maintain a null energy balance; therefore, for a constant operating time:

$$\begin{aligned} C_{el} &= psh + f_P t_w^{ef} \rightarrow C_{el} = \frac{\xi_{el}}{P_{PV} t_{op}};\ f_P = \frac{P_w}{P_{PV}} \\ C_{th} &= G + C_o COP \rightarrow C_{th} = \frac{\xi_{th}}{\eta_{th} S t_{op}} - \frac{\dot{m}_b}{\eta_{th} S} LHV;\ C_2 = \frac{P_g^{el}}{\eta_{th} S} \end{aligned} \tag{5}$$

Since C_{el}, C_{th}, and C_o are constant, the AI protocol adjusts twef as the solar radiation changes; thus, the psh value, to maintain the electric energy balance null. A similar procedure applies for the thermal energy balance, with the AI protocol modifying the geothermal COP value as the solar radiation changes.

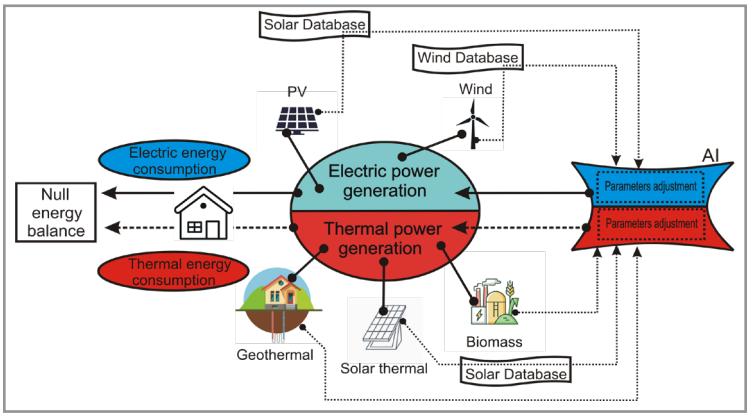

Figure 9: Flowchart for the Electric and Thermal Energy Supply AI Protocol Subroutine

Electric Energy

Because the addition of solar photovoltaic and wind energy may produce more power than required, the AI protocol prioritizes renewable resource use depending on the system's efficiency.

Based on this statement, the control unit evaluates the PV array and wind turbine performance when operating at specific energy requirement conditions; in such a case, considering the instantaneous power demand, P_i, and the photovoltaic and wind power generation, we have:

$$\eta^s = \frac{P_i^s}{P_{max}^s} \quad (6)$$

Superscript s accounts for the source type, photovoltaic or wind, and subscript max corresponds to the source peak power.

The power source selection depends on the energy demand coverage factor; if the power source supplies more energy than required, the efficiency criterion applies; otherwise, the AI protocol selects the most efficient power source to provide all available power and regulates the other power source to supply the remaining energy to achieve a null energy balance. Figure 10 shows the flowchart for this AI protocol subroutine.

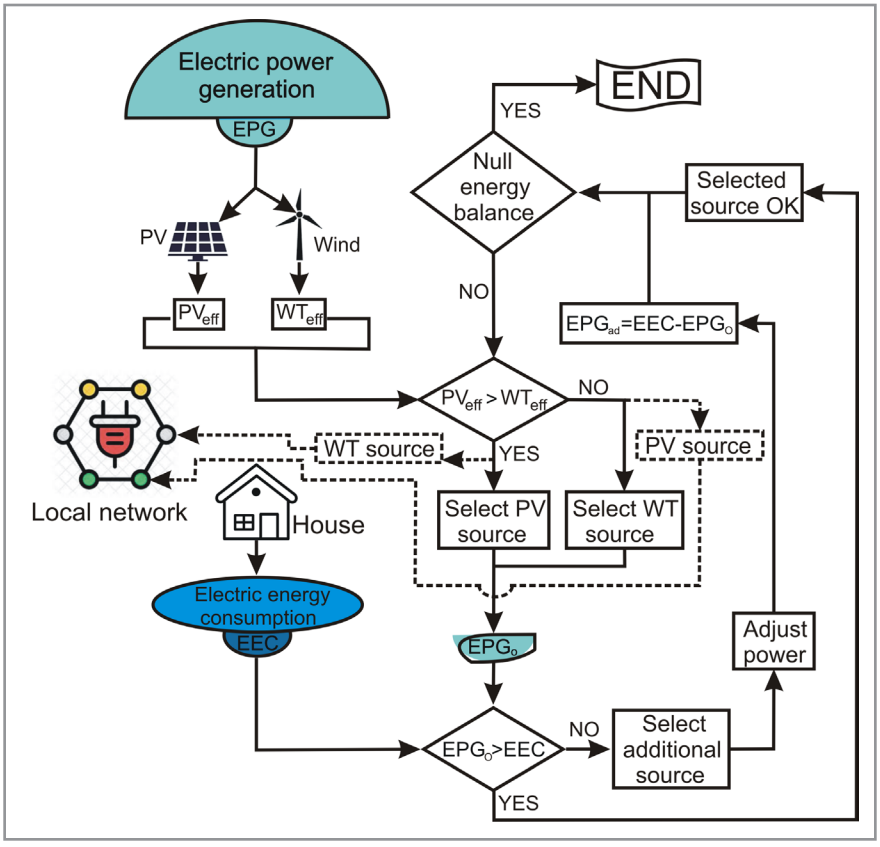

Figure 10: Flowchart of the AI Control Protocol Subroutine for Power Source Selection and Adjustment in the Electric Energy Supply Case

Since the PV panel operates at the maximum efficiency possible due to the integrated Maximum Power Point Tracking device, the PV output power, P^{out}_{PV}, only depends on the solar radiation value according to the expression:

$$P^{out}_{PV} = P^{o}_{PV}\frac{G}{G_o} \tag{7}$$

P^{o}_{PV} is the maximum PV output power at the maximum solar radiation, G_o=1 kW/m2. G is the current incoming solar radiation.

The block diagram of Figure 10 only applies to households where solar photovoltaic or wind systems exist; otherwise, the household electric energy supply depends on the local network, houses 7 and 8, in our study.

When the two power sources are active, if the AI protocol selects only one, the AI protocol commands the control unit to derive the energy produced by the non-selected source to the local network, as shown in Figure 10.

The AI protocol predicts which power source should be connected at any given time based on the detected consumption and performance data stored in the system database. This procedure optimizes the local network performance since it preserves the most efficient power generation for the household installation where energy is produced, releasing the power generation residue to the local network and minimizing energy losses.

Considering two houses with power demand Ph1 and Ph2, covered by the PV array or the wind turbine, the following equation applies:

$$P_{hi} = \eta_{PVi}P^{o}_{PVi} = \eta_{WTi}P^{o}_{WTi} \tag{8}$$

Subscript i applies indistinctively for any of the two houses.

If one of the power sources operates at higher efficiency than the other, $\eta_{PV1}>\eta_{WT1}$ for house number 1, and $\eta_{PV2}<\eta_{WT2}$ for house number 2, for equal PV array and wind turbine output power, Equation 8 transforms into:

$$\eta_{PV1}P^{o}_{PV1} > \eta_{WT1}P^{o}_{WT1}$$
$$\eta_{PV2}P^{o}_{PV2} < \eta_{WT2}P^{o}_{WT2} \tag{9}$$

Sub-indexes 1 and 2 account for houses 1 and 2.

Considering $\eta_{PV1}=\eta_{WT1}+\Delta\eta_{WT1}$ (10), and $\eta_{WT2}=\eta_{PV2}+\Delta\eta_{PV2}$ (11), using Equation 9 and operating:

$$P_{WT1}+\Delta\eta_{WT1}P^{o}_{WT1} = P_{PV2}+\Delta\eta_{PV2}P^{o}_{PV2} \tag{12}$$

Applying Equation 8 for both houses:

$$P_{WT1} = \eta_{WT1}P^{o}_{WT1} = \eta_{PV2}P^{o}_{PV2} = P_{PV2} \tag{13}$$

Combining Equations 10 to 13:

$$\frac{\eta_{PV1}}{\eta_{WT1}} = \frac{\eta_{WT2}}{\eta_{PV2}} \tag{14}$$

Applying Equation 14 to any household combination, we have:

$$\prod_{i=1}^{n}\eta_{zi} = K \tag{15}$$

K is a constant and Π is the producing mathematical operator.

Equation 15 shows the algorithm that the AI protocol uses to optimize the energy transfer between adjacent houses to maintain energy balance null.

When dealing with the local network, the AI protocol develops a mathematical approach method to achieve the highest efficiency possible in the energy transfer because Equation 15 does not fulfill every pair of adjacent houses. The approaching method considers all the local network households exchanging energy between all of them, making the derivative of the sum of the relationship between the efficiencies of the power sources zero; mathematically:

$$d\left(\sum_{i,j=1}^{n}\frac{\eta_{zi}}{\eta_{zj}}\right) = 0 \tag{16}$$

Developing Equation 16:

$$\sum_{i,j=1}^{n}\frac{\eta_{zi}\Delta\eta_{zj}-\eta_{zj}\Delta\eta_{zi}}{\eta^{2}_{zi}} + \sum_{i,j=1}^{n}\frac{\eta_{zj}\Delta\eta_{zi}-\eta_{zi}\Delta\eta_{zj}}{\eta^{2}_{zj}} = 0 \tag{17}$$

Equation 17 represents the algorithm the AI protocol uses to optimize the electric energy transfer when all houses of the local network exchange energy between them all.

If only one power source exists, the Figure 11 flowchart applies. Figure 11 represents the flowchart for a PV array as a power source but also applies to wind energy. The AI protocol operates similarly by replacing the PV source with the wind one (shown in a dashed circle).

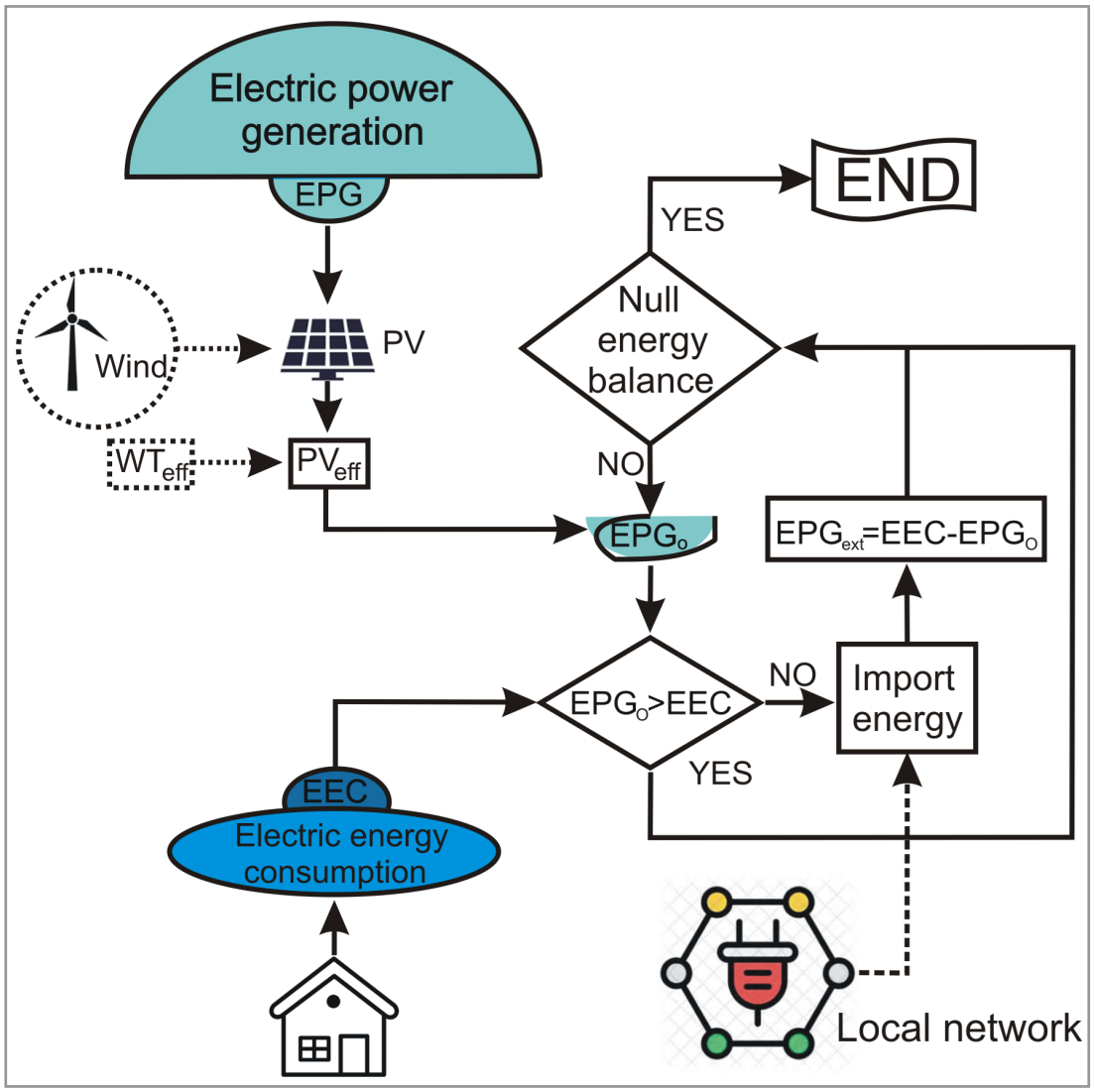

Figure 11: Flowchart of the AI Control Protocol Subroutine for Single Power Source Electric Energy Supply Case

The mathematical approach method developed for two power sources is valid for a single one with the algorithm modified as follows:

$$\sum_{i,j=1}^{m} \frac{\eta_{si}\Delta\eta_{sj} - \eta_{sj}\Delta\eta_{si}}{\eta_{si}^2} + \sum_{i,j=1}^{n} \frac{\eta_{sj}\Delta\eta_{si} - \eta_{si}\Delta\eta_{sj}}{\eta_{sj}^2} + \sum_{k=m-n}^{n} \frac{1}{\eta_{sk}} = 0 \quad (18)$$

Subscripts i and j account for the two power sources in households with PV and wind installations; subscript k accounts for the single power source in houses with a PV array or wind turbine system. Super and subscript m in the summations correspond to the number of houses with two power sources.

Thermal Energy

Thermal energy generation, consumption, and distribution follow identical analysis as for the electric energy with the only difference that up to three power sources may intervene in the power generation and energy distribution via local network. Equation 6 applies changing the superscript s by t with t accounting for solar thermal, biomass, and geothermal.

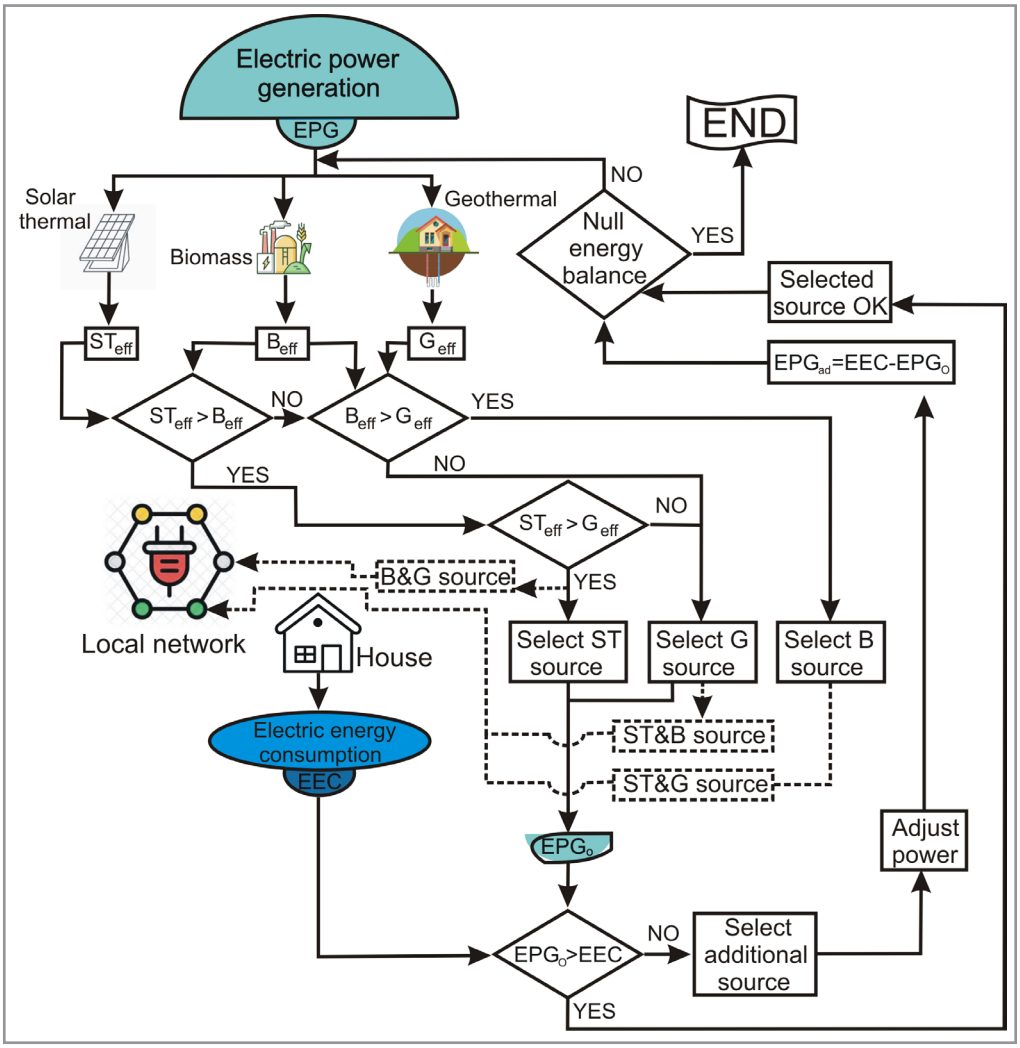

Figure 12: Flowchart of the AI Control Protocol Subroutine for Power Source Selection and Adjustment in the Thermal Energy Supply Case

Replicating the power analysis for the electric energy generation system, Equation 15 applies with the only difference that the subscript snow applies to solar thermal (ST), biomass (B), and geothermal (G); therefore, Equation 16 converts into:

$$d\left(\sum_{i,j=1}^{n}\frac{\eta_{zi}}{\eta_{zj}}+\sum_{i,k=1}^{n}\frac{\eta_{zi}}{\eta_{zk}}+\sum_{j,k=1}^{n}\frac{\eta_{zj}}{\eta_{zk}}\right)=0 \quad (19)$$

Developing Equation 19:

$$\sum_{i,j=1}^{n}\frac{\eta_{zi}\Delta\eta_{zj}-\eta_{zj}\Delta\eta_{zi}}{\eta_{zi}^2}+\sum_{i,j=1}^{n}\frac{\eta_{zj}\Delta\eta_{zi}-\eta_{zi}\Delta\eta_{zj}}{\eta_{zj}^2}+\sum_{i,k=1}^{n}\frac{\eta_{zi}\Delta\eta_{zk}-\eta_{zk}\Delta\eta_{zi}}{\eta_{zi}^2}+$$
$$+\sum_{i,k=1}^{n}\frac{\eta_{zk}\Delta\eta_{zi}-\eta_{zi}\Delta\eta_{zk}}{\eta_{zk}^2}+\sum_{j,k=1}^{n}\frac{\eta_{zj}\Delta\eta_{zk}-\eta_{zk}\Delta\eta_{zj}}{\eta_{zj}^2}+\sum_{j,k=1}^{n}\frac{\eta_{zk}\Delta\eta_{zj}-\eta_{zj}\Delta\eta_{zk}}{\eta_{zk}^2}=0 \quad (20)$$

Equation 20 represents the algorithm the AI protocol uses to optimize the thermal energy transfer when all houses of the local network exchange energy between them all.

If only two of the three power sources exist, the Figure 11 flowchart applies replacing PV and Wind by ST and B, ST and G, or B and G, depending on which pair of sources are active.

If we deal with a single power source, the analysis is identical to the one developed for the electric energy system with the only difference that Equation 18 converts into:

$$\sum_{i,j=1}^{n}\frac{\eta_{zi}\Delta\eta_{zj}-\eta_{zj}\Delta\eta_{zi}}{\eta_{zi}^2}+\sum_{i,j=1}^{n}\frac{\eta_{zj}\Delta\eta_{zi}-\eta_{zi}\Delta\eta_{zj}}{\eta_{zj}^2}+\sum_{i,k=1}^{n}\frac{\eta_{zi}\Delta\eta_{zk}-\eta_{zk}\Delta\eta_{zi}}{\eta_{zi}^2}+$$
$$+\sum_{i,k=1}^{n}\frac{\eta_{zk}\Delta\eta_{zi}-\eta_{zi}\Delta\eta_{zk}}{\eta_{zk}^2}+\sum_{j,k=1}^{n}\frac{\eta_{zj}\Delta\eta_{zk}-\eta_{zk}\Delta\eta_{zj}}{\eta_{zj}^2}+\sum_{j,k=1}^{n}\frac{\eta_{zk}\Delta\eta_{zj}-\eta_{zj}\Delta\eta_{zk}}{\eta_{zk}^2}+\sum_{i=m=n}^{n}\frac{1}{\eta_{zi}}=0 \quad (21)$$

The Artificial Intelligence protocol collects data on performance, η, and efficiency variation, Δη, from the control unit, which receives data from the power controller sensors, replacing calculated values in the corresponding algorithms to make decisions on the energy transfer throughout the local network.

Experimental Results

Based on the premise of null energy balance, the AI protocol is submitted to a verification process to validate the accuracy of the proposed methodology predictions. The verification process consists of developing experimental tests run on the local network households, collecting daily hourly data from current photovol-

taic and wind power generation, and comparing the experimental data with the predicted values from the AI protocol algorithms.

The AI protocol evaluates the daily hourly energy generation for every household, splitting data into two groups: the one including the hourly periods where the energy balance is above zero and the one corresponding to negative energy balance hourly periods.

The verification procedure compares the energy generation experimental data collected from the individual household power controller with the predicted values by the AI protocol corresponding to the positive energy balance group.

The developed process is applied to the every house of the local network to verify the validity of the AI protocol. The experimental study includes two sections: first, electric and thermal power generation comparison, and second, evaluation of the energy transfer for null energy balance premise fulfillment.

Power Generation

Electric Energy

The test starts with the verification of electric power generation using installation power data from Table 1, and solar and wind resource daily hourly evolution (Figure 4),. Photovoltaic array and wind turbine efficiency derive from the daily hourly power generation and the peak power generation corresponding to the energy resource for every source. Peak power generation depends on the selected type of PV panel and wind turbine for the household installation, and current power generation comes from the power analyzer device installed in every house.

The photovoltaic and wind system efficiency are drawn in Figure 13. It should be noticed that graphs only show the existing power source efficiency. Houses 7 and 8 do not appear since they do not have photovoltaic or wind installation.

The power factor is calculated as the ratio between the current output power and the device peak power, photovoltaic panel or wind turbine.

The reader should notice that the power factor is low for some cases, like the photovoltaic system in house 3 where it barely achieves a 6% at the maximum, or in house 4 where the wind power system operates at a maximum power factor of 6%, and the PV system between 6% and 16%.

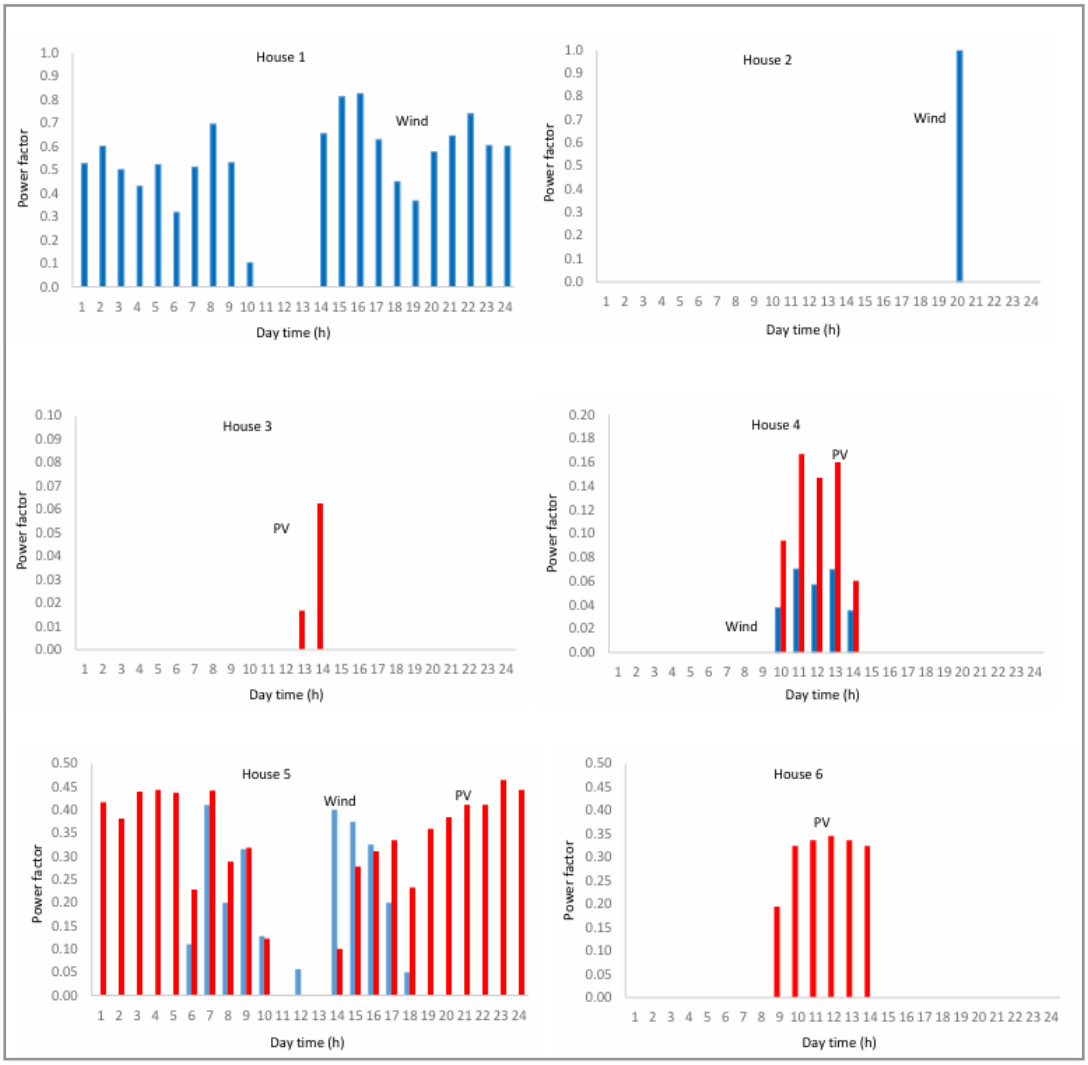

Figure 13: Hourly Distribution of Individual House Solar Photovoltaic and Wind System Power Factor for a Typical Day

The results show a lack of adequate sizing of the power installation, both photovoltaic and wind; this is because the homes were initially designed to adjust generation to demand, but the change in the number of people living in the different homes, as well as the modification of the consumption habits of the residents have given rise to this mismatch between generation and consumption, which causes a very low power factor in some cases.

This particular circumstance is the reason for having proposed the use of a local network for the exchange of electrical energy between the different homes governed by a control system that relies on an Artificial Intelligence protocol to optimize said energy exchange and operate the local network as a joint Distributed Generation system without dependence on the network.

Theoretical energy generation is determined applying Equation 22:

$$\xi_{el} = f_{pv} P_{pv} psh + f_w P_w t_w^{ef} \quad (22)$$

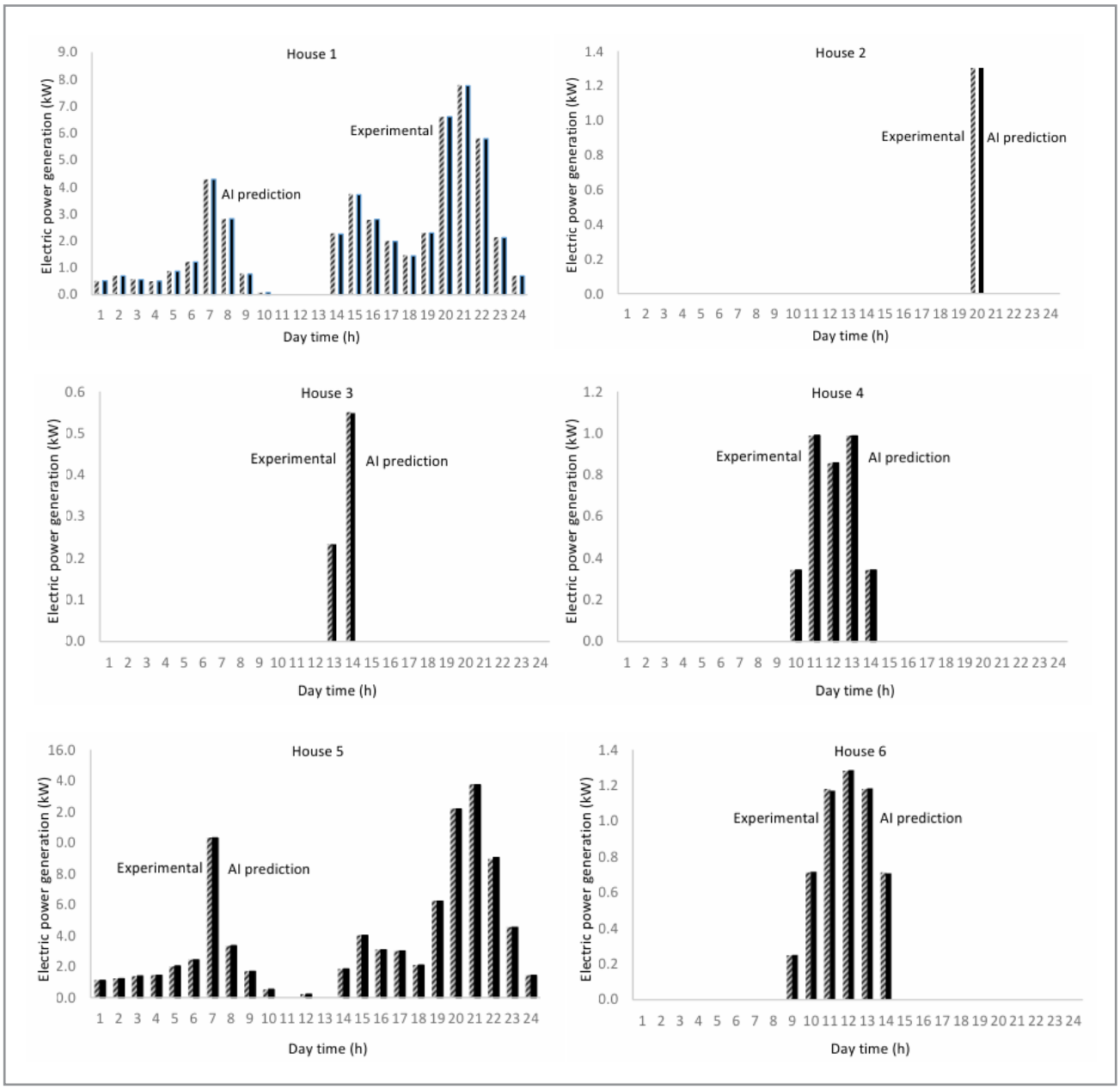

Figure 14: Comparative Analysis of Daily Hourly Household Electric Energy Generation: AI Protocol Predicted Value (Solid Bar); Experimental Data (Dashed Bar)

Since the AI protocol works on the null energy balance premise, the predicted value by the AI protocol should match the experimental data. We observe that AI prediction and experimental data match within high accuracy. Table 5 shows the matching index between both values.

Table 5: Matching Index Between AI Prediction and Experimental Data for Electric Power Generation in the Individual Houses of the Local Network

House	1	2	3	4	5	6
σ	1.0016	1.0000	1.0003	0.9997	1.0001	0.9999

The data analysis in Table 5 show the perfect matching between AI prediction and experimental values, higher than 99.7% on average, proving the validity of the AI protocol.

Thermal Energy

Repeating the process for the thermal energy and applying Equation 6, we obtain the power factor adapted for every thermal power source (Figure 15).

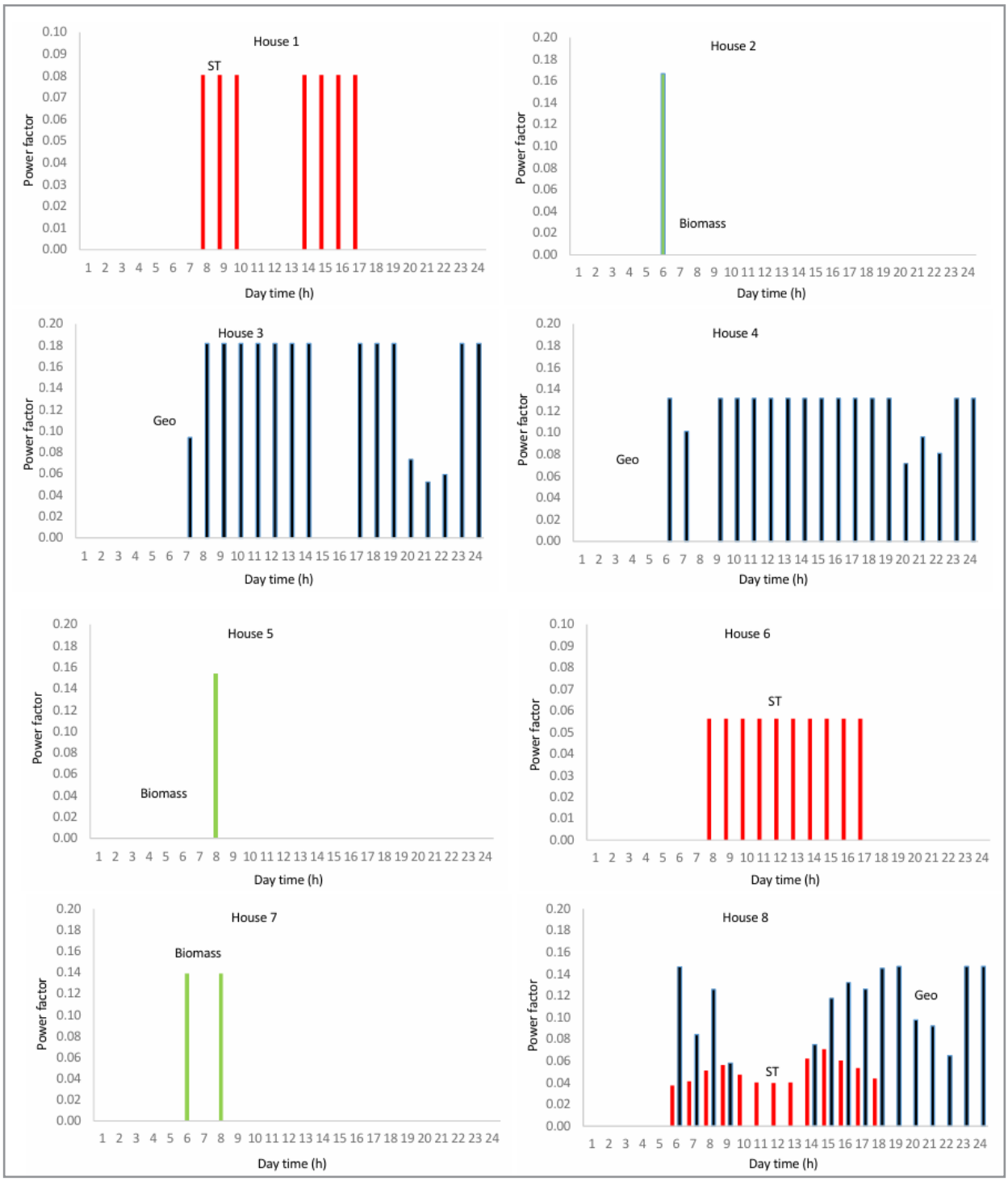

Figure 15: Hourly Distribution of Individual House Solar Thermal, Biomass and-Geothermal System Power Factor for a Typical Day

As in the case of electric power generation, thermal power sources are poorly sized for the current energy demand; the reason is similar to the one exposed in the electric power generation analysis: different numbers of residents in every house together with changes in energy consumption habits.

The information about the original power source design for every house shows that they depended on owners' likes, purchasing power and investment costs, space availability, and some other factors that conditioned the power source installation design and size.

Similarly to electric power generation, the mismatching between thermal power generation and energy demand represents a unique opportunity to apply the artificial intelligence protocol to a control unit for energy exchange between houses, making the local network operate as a district heating, achieving a null energy balance, if possible, limiting the dependence on external sources like fossil fuels (gas, coal), and optimizing the local network thermal global performance.

Now, reproducing the comparative analysis between AI predictions and experimental results for thermal energy, we have (Figure 16):

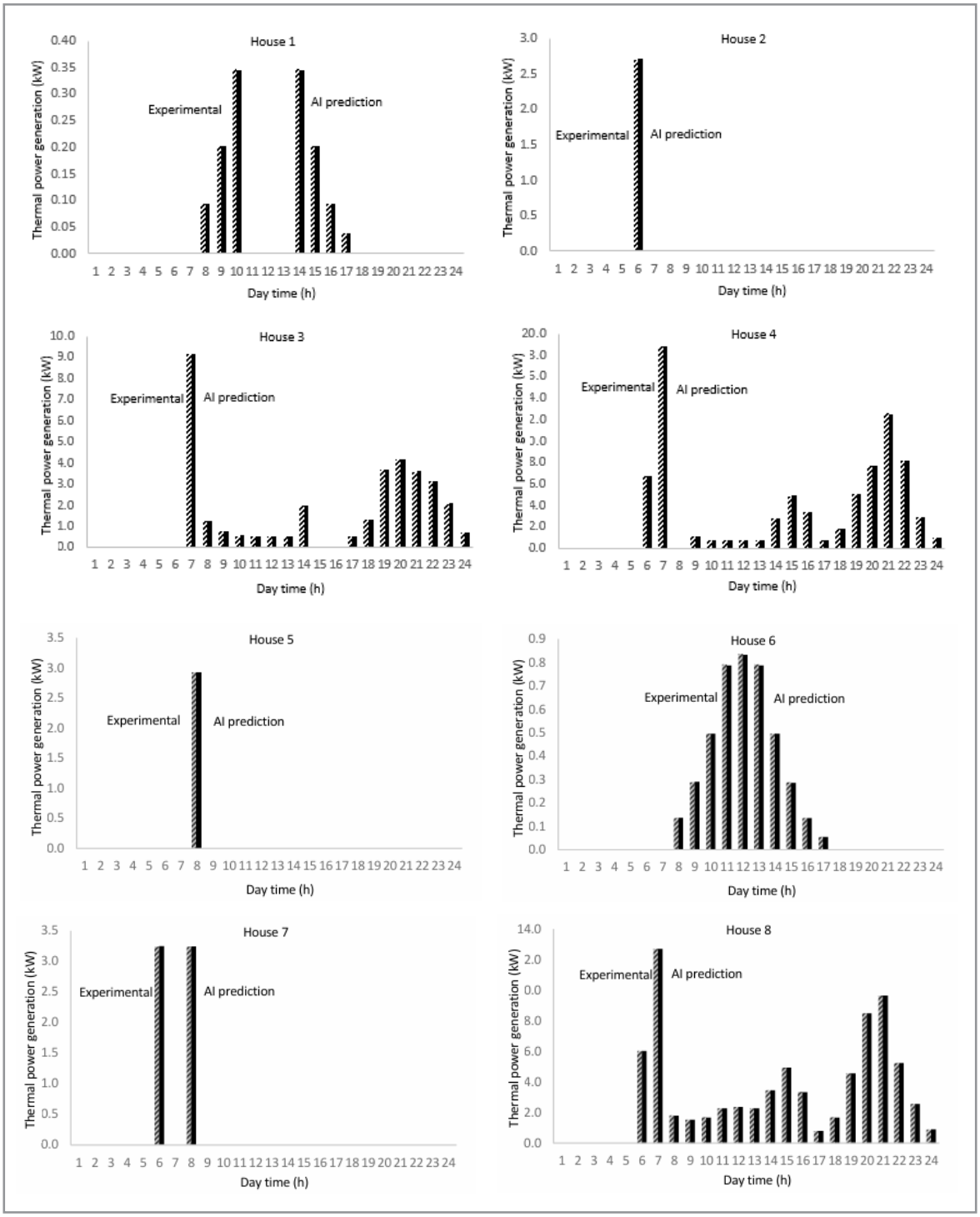

Figure 16: Comparative Analysis of Daily Hourly Household Thermal Energy Generation: AI Protocol Predicted Value (Solid Bar); Experimental Data (Dashed Bar)

As in the case of electric energy, the AI protocol predicts thermal power generation with high accuracy, matching the experimental data as shown in Figure 16. The experimental data are collected by the control unit, which receives information from the thermal power analyzer installed in every household installation. Table 6 shows the matching index between the AI-predicted values and experimental data for thermal power generation in every house of the local network.

Table 6: Matching Index Between AI Prediction and Experimental Data for Thermal Power Generation in the Individual Houses of the Local Network

House	1	2	3	4	5	6	7	8
σ	0.9996	1.0002	1.0007	1.0015	1.0001	1.0001	1.0002	0.9996

The data analysis in Table 6 show the perfect matching between AI prediction and experimental values, higher than 99.8% on average, proving the validity of the AI protocol.

Energy Balance

We design the AI protocol to predict system performance based on the premise of a null energy balance for the local network. The AI protocol also includes a subroutine to optimize the performance, selecting the most efficient power source to exchange energy between houses when individual house energy balance is not null.

If only a power source exists, electric or thermal, the AI protocol subroutine does not make any decision about the selected power source; however, if more than one operates in an individual installation, the AI protocol applies the power selection decision as shown in Figures 10 and 12 for electric and thermal energy.

The second part of the experimental tests aims to verify the previous statement; to this goal, we focused the analysis on houses 4 and 5 for electric energy and 8 for thermal since they are equipped with double power sources. Figure 17 shows the results of applying the AI protocol to the selected houses.

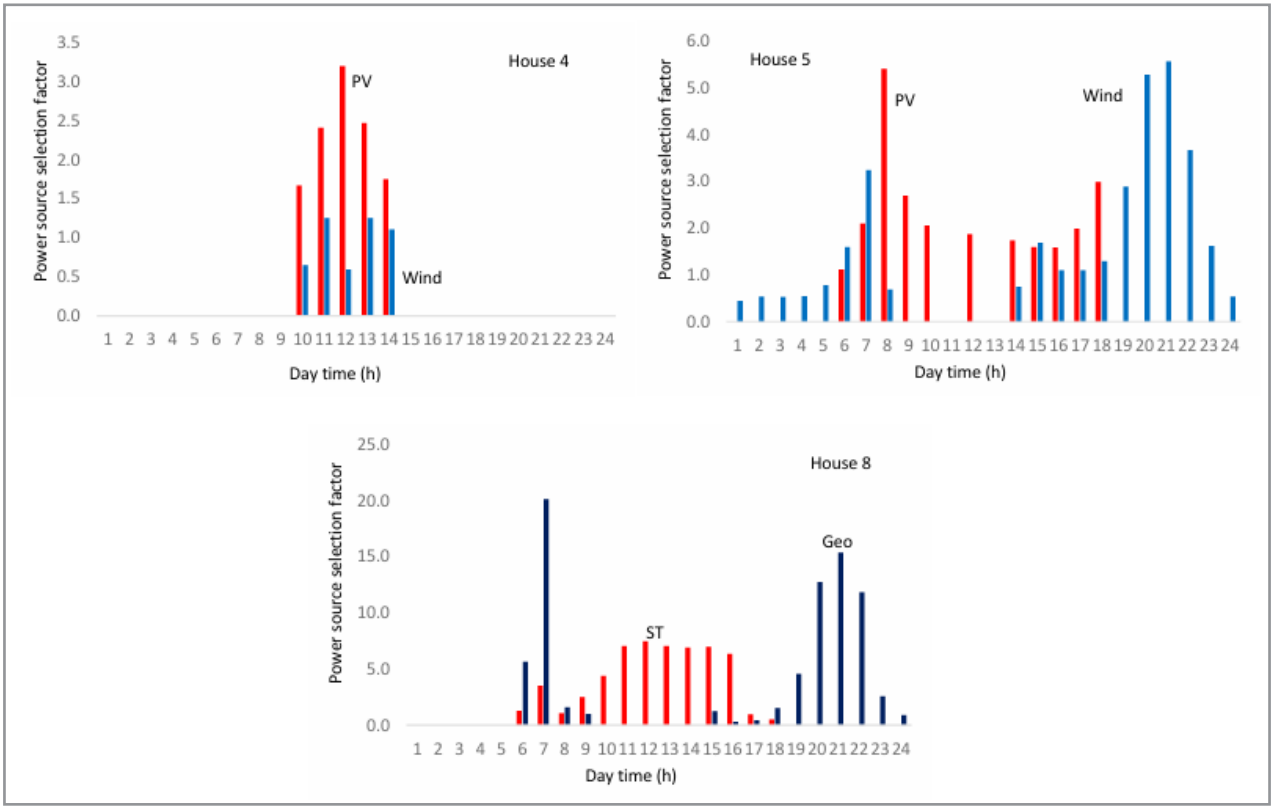

Figure 17: Power Source Selection Factor Based on AI Protocol. Upper Section: Electric Energy Installation; Lower Section: Thermal Energy Installation

Analyzing data in Figure 17, we notice that the AI protocol assigns a factor to every operating power source; based on this factor, the AI protocol commands the control unit to open the exchange energy from the selected power source household to the electric network distributor or the heat distribution ring. The assigned selection factor is based on the null energy balance premise and corresponds to the power generation weighted value that makes the energy balance null.

When the selection factor is non-null for any power source during the same hourly interval, the AI protocol prioritizes the source with the higher factor. It utilizes any additional power

source to supplement the energy supplied by the primary source until the energy balance reaches zero. For instance, in the case of house 4, during the interval from 10 am to 2 pm, the protocol prioritizes the photovoltaic power source due to its superior efficiency, using wind energy to supplement the default energy until a null energy balance is achieved.

In the case of house 5 for electric energy, we observe that the AI protocol exchanges between photovoltaic and wind power sources depending on which one is more efficient. For the hourly intervals at 6 am, 7 am, and 3 pm, the AI prioritizes the wind power source as the most efficient; however, at 8 am, and 2, 5, and 6 pm, is the photovoltaic the selected power source as the most efficient.

The time intervals where a selection factor appears for only one power source means that the other source is unnecessary to achieve the null energy balance. Similarly, no power source is necessary for the energy exchange process if no selection factor appears.

The analysis for the thermal energy case, house 8, is identical to the electric energy case for house 5. Figure 18 shows the results for the energy balance applying the AI protocol to the local network.

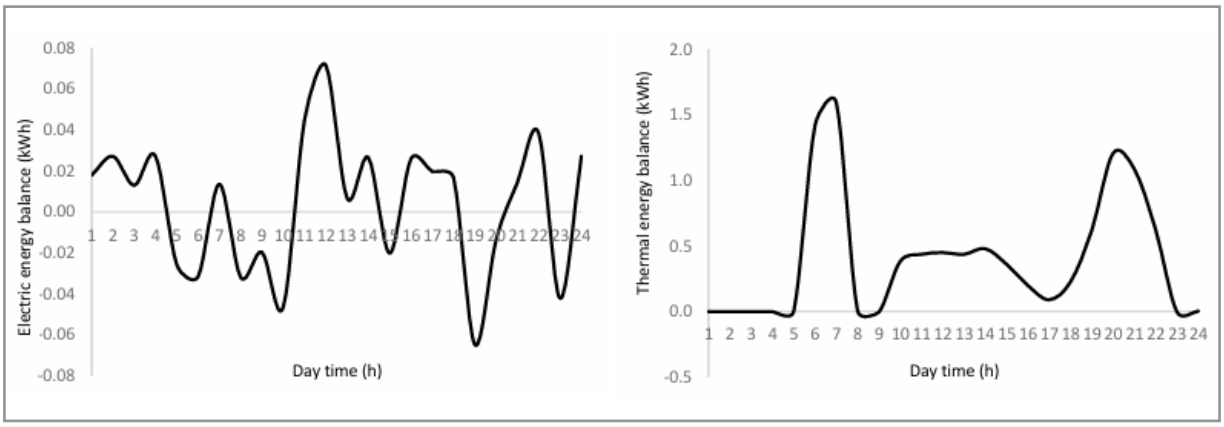

Figure 18: Daily Hourly Energy Balance for the Local Network. Left Side: Electric; Right Side: Thermal

The data analysis from Figure 18 shows a negligible energy balance deviation from the zero value, with a maximum difference of 0.07 kWh for the electric energy and 1.60 kWh for the thermal energy, proving the validity of the AI protocol application to the energy management control of the local network.

We notice that in the electric energy case, the global energy balance throughout the day is almost null, 0.10 kWh/day, while in the case of thermal energy, the daily balance is 9.61 kWh/day. This deviation respect to the null energy balance condition is due to thermal losses during heat transportation across the heat distribution network. Considering the daily global energy transfer in the local network, 209 kWh/day, thermal losses represent 4.6% of the total, an acceptable value for the heat transfer process.

Conclusions

An artificial intelligence protocol (AIP) to command a control unit for energy management in a local network is designed and developed. The AIP operates based on the null energy balance premise, making the local network independent on the grid. The AIP protocol applies to a group of households powered by renewable energies, photovoltaic and wind for electric generation, and solar thermal, biomass, and geothermal for heat production.

The AIP predicts the daily hourly electric and thermal power generation within high accuracy, prioritizing the most efficient power source to supply energy to the individual installation and to exchange energy with other household installation operating in energy default state. The AIP may select or not a power source for energy exchange depending on the energy balance and power supply by the selected power source; therefore, the AIP can disconnect a household power source from the local network energy distribution if the selected power source makes the local network to achieve a null energy balance.

The AIP has been tested in a group of households with severe individual energy unbalance to prove the validity of the energy management process. The results of the experimental tests showed that the AIP predictions match experimental values within 99.8% accuracy for the electric energy and 97.1% for the thermal. Furthermore, the daily hourly local network energy balance is near zero deviation regarding the null value, with a maximum difference of 0.07 kWh, meaning a standard deviation lower than 0.21% for the electric energy, and 2.94% for thermal case.

The AIP provides a practical tool for energy network designers and managers to optimize the system performance, improving the energy supply by selecting the most efficient power source for the local network energy exchange.

References

1. Henning, H. M., & Palzer, A. (2014). A comprehensive model for the German electricity and heat sector in a future energy system with a dominant contribution from renewable energy technologies-Part I: Methodology. Renewable and Sustainable Energy Reviews, 30, 1003-1018.

2. Sioshansi, F. (Ed.). (2011). Smart grid: integrating renewable, distributed and efficient energy. Academic Press.
3. Tamoor, M., Abu Bakar Tahir, M., Zaka, M. A., & Iqtidar, E. (2022). Photovoltaic distributed generation integrated electrical distribution system for development of sustainable energy using reliability assessment indices and levelized cost of electricity. Environmental Progress & Sustainable Energy, 41(4), e13815.
4. Erge, T., Hoffmann, V. U., & Kiefer, K. (2001). The German experience with grid-connected PV-systems. Solar Energy, 70(6), 479-487.
5. de Faria Jr, H., Trigoso, F. B., & Cavalcanti, J. A. (2017). Review of distributed generation with photovoltaic grid connected systems in Brazil: Challenges and prospects. Renewable and Sustainable Energy Reviews, 75, 469-475.
6. Child, M., Kemfert, C., Bogdanov, D., & Breyer, C. (2019). Flexible electricity generation, grid exchange and storage for the transition to a 100% renewable energy system in Europe. Renewable energy, 139, 80-101.
7. Argiriou, A. A., & Mirasgedis, S. (2003). The solar thermal market in Greece-review and perspectives. Renewable and Sustainable Energy Reviews, 7(5), 397-418.
8. Weiss, W. (2003). Solar heating systems for houses: a design handbook for solar combisystems. Earthscan.
9. Bać, A., Nemś, M., Nemś, A., & Kasperski, J. (2019). Sustainable integration of a solar heating system into a single-family house in the climate of Central Europe-A case study. Sustainability, 11(15), 4167.
10. D'Agostino, D., Minichiello, F., & Valentino, A. (2020). Contribution of low enthalpy geothermal energy in the retrofit of a single-family house: a comparison between two technologies. Journal of Advanced Thermal Science Research, 7, 30-39.
11. D'Agostino, D., Minichiello, F., Petito, F., Renno, C., & Valentino, A. (2022). Retrofit strategies to obtain a NZEB using low enthalpy geothermal energy systems. Energy, 239, 122307.
12. Bleicher, A., & Gross, M. (2016). Geothermal heat pumps and the vagaries of subterranean geology: Energy independence at a household level as a real world experiment. Renewable and Sustainable Energy Reviews, 64, 279-288.
13. Ilisei, G., Catalina, T., Alexandru, M., & Gavriliuc, R. (2019). Implementation of a geothermal heat pump system in a solar passive house. In E3S Web of Conferences (Vol. 85, p. 07014). EDP Sciences.
14. Palomba, V., Borri, E., Charalampidis, A., Frazzica, A., Cabeza, L. F., & Karellas, S. (2020). Implementation of a solar-biomass system for multi-family houses: Towards 100% renewable energy utilization. Renewable energy, 166, 190-209.
15. Las-Heras-Casas, J., López-Ochoa, L. M., Paredes-Sánchez, J. P., & López-González, L. M. (2018). Implementation of biomass boilers for heating and domestic hot water in multi-family buildings in Spain: Energy, environmental, and economic assessment. Journal of Cleaner Production, 176, 590-603.
16. Wöhler, M., Andersen, J. S., Becker, G., Persson, H., Reichert, G., Schön, C., ... & Pelz, S. K. (2016). Investigation of real life operation of biomass room heating appliances–Results of a European survey. Applied Energy, 169, 240-249.
17. Bessa, R., Moreira, C., Silva, B., & Matos, M. (2019). Handling renewable energy variability and uncertainty in power system operation. Advances in Energy Systems: The Large-scale Renewable Energy Integration Challenge, 1-26.
18. Sinsel, S. R., Riemke, R. L., & Hoffmann, V. H. (2020). Challenges and solution technologies for the integration of variable renewable energy sources—a review. renewable energy, 145, 2271-2285.
19. Lund, P. D., Lindgren, J., Mikkola, J., & Salpakari, J. (2015). Review of energy system flexibility measures to enable high levels of variable renewable electricity. Renewable and sustainable energy reviews, 45, 785-807.
20. Beaudin, M., Zareipour, H., Schellenberglabe, A., & Rosehart, W. (2010). Energy storage for mitigating the variability of renewable electricity sources: An updated review. Energy for sustainable development, 14(4), 302-314.
21. Ouramdane, O., Elbouchikhi, E., Amirat, Y., Le Gall, F., & Sedgh Gooya, E. (2022). Home energy management considering renewable resources, energy storage, and an electric vehicle as a backup. Energies, 15(8), 2830.
22. Suberu, M. Y., Mustafa, M. W., & Bashir, N. (2014). Energy storage systems for renewable energy power sector integration and mitigation of intermittency. Renewable and Sustainable Energy Reviews, 35, 499-514.
23. Child, M., Kemfert, C., Bogdanov, D., & Breyer, C. (2019). Flexible electricity generation, grid exchange and storage for the transition to a 100% renewable energy system in Europe. Renewable energy, 139, 80-101.
24. Mulder, G., De Ridder, F., & Six, D. (2010). Electricity storage for grid-connected household dwellings with PV panels. Solar energy, 84(7), 1284-1293.
25. Velik, R. (2013). Battery storage versus neighbourhood energy exchange to maximize local photovoltaics energy consumption in grid-connected residential neighbourhoods. IJARER International Journal of Advanced Renewable Energy Research, 2(6).
26. Bhatnagar, D., Currier, A. B., Hernandez, J., Ma, O., & Kirby, B. (2013). Market and policy barriers to energy storage deployment (No. SAND2013-7606). Sandia National Lab.(SNL-NM), Albuquerque, NM (United States); United States., Washington, DC.
27. Parra, D., Swierczynski, M., Stroe, D. I., Norman, S. A., Abdon, A., Worlitschek, J., ... & Patel, M. K. (2017). An interdisciplinary review of energy storage for communities: Challenges and perspectives. Renewable and Sustainable Energy Reviews, 79, 730-749.
28. Sioshansi, R., Denholm, P., & Jenkin, T. (2012). Market and policy barriers to deployment of energy storage. Economics of Energy & Environmental Policy, 1(2), 47-64.
29. Mogrovejo-Narvaez, M., Barragán-Escandón, A., Zalamea-León, E., & Serrano-Guerrero, X. (2024). Barriers to the Implementation of On-Grid Photovoltaic Systems in Ecuador. Sustainability, 16(21), 9466.
30. Palm, J. (2018). Household installation of solar panels–Motives and barriers in a 10-year perspective. Energy Policy, 113, 1-8.
31. Nadeem, T. B., Siddiqui, M., Khalid, M., & Asif, M. (2023). Distributed energy systems: A review of classification, technologies, applications, and policies. Energy Strategy Reviews, 48, 101096.

32. Lund, H., Möller, B., Mathiesen, B. V., & Dyrelund, A. (2010). The role of district heating in future renewable energy systems. Energy, 35(3), 1381-1390.
33. Heiskanen, E., & Matschoss, K. (2017). Understanding the uneven diffusion of building-scale renewable energy systems: A review of household, local and country level factors in diverse European countries. Renewable and Sustainable Energy Reviews, 75, 580-591.
34. Kostevšek, A., Cizelj, L., Petek, J., & Pivec, A. (2013). A novel concept for a renewable network within municipal energy systems. Renewable energy, 60, 79-87.
35. Koirala, B. P., van Oost, E., & van der Windt, H. (2018). Community energy storage: A responsible innovation towards a sustainable energy system?. Applied energy, 231, 570-585.
36. Niemi, R., Mikkola, J., & Lund, P. D. (2012). Urban energy systems with smart multi-carrier energy networks and renewable energy generation. Renewable energy, 48, 524-536.
37. Tomc, E., & Vassallo, A. M. (2016). The effect of individual and communal electricity generation, consumption and storage on urban Community Renewable Energy Networks (CREN): an Australian case study. International Journal of Sustainable Energy Planning and Management, 11, 15-32.
38. Parikh, P. (2009). Distribution system automation. University of Western Ontario: Electrical and Computer Engineering Department. Course Project Report. Ontario.
39. Lopes, M., Antunes, C. H., Soares, A. R., Carreiro, A., Rodrigues, F., Livengood, D., ... & Peixoto, P. (2012, May). An automated energy management system in a smart grid context. In 2012 IEEE International Symposium on Sustainable Systems and Technology (ISSST) (pp. 1-1). IEEE.
40. Zafar, U., Bayhan, S., & Sanfilippo, A. (2020). Home energy management system concepts, configurations, and technologies for the smart grid. IEEE access, 8, 119271-119286.
41. Rathor, S. K., & Saxena, D. (2020). Energy management system for smart grid: An overview and key issues. International Journal of Energy Research, 44(6), 4067-4109.
42. Omitaomu, O. A., & Niu, H. (2021). Artificial intelligence techniques in smart grid: A survey. Smart Cities, 4(2), 548-568.
43. Bose, B. K. (2017). Artificial intelligence techniques in smart grid and renewable energy systems—some example applications. Proceedings of the IEEE, 105(11), 2262-2273.
44. Noviati, N. D., Maulina, S. D., & Smith, S. (2024). Smart grids: Integrating ai for efficient renewable energy utilization. International Transactions on Artificial Intelligence, 3(1), 1-10.